Acta Crystallographica Section D
Biological Crystallography
ISSN 0907-4449

Proline: Mother Nature's cryoprotectant applied to protein crystallography

Travis A. Pemberton,[a] Brady R. Still,[a] Emily M. Christensen,[a] Harkewal Singh,[a] Dhiraj Srivastava[a] and John J. Tanner[a,b]*

[a]Department of Chemistry, University of Missouri-Columbia, Columbia, MO 65211, USA, and [b]Department of Biochemistry, University of Missouri-Columbia, Columbia, MO 65211, USA

Correspondence e-mail: tannerjj@missouri.edu

Received 13 March 2012
Accepted 1 May 2012

PDB References: lysozyme, 4e3u; xylose isomerase, 4e3v; histidine acid phosphatase, 4e3w; 1-pyrroline-5-carboxylate dehydrogenase, 4e3x.

L-Proline is one of Mother Nature's cryoprotectants. Plants and yeast accumulate proline under freeze-induced stress and the use of proline in the cryopreservation of biological samples is well established. Here, it is shown that L-proline is also a useful cryoprotectant for protein crystallography. Proline was used to prepare crystals of lysozyme, xylose isomerase, histidine acid phosphatase and 1-pyrroline-5-carboxylate dehydrogenase for low-temperature data collection. The crystallization solutions in these test cases included the commonly used precipitants ammonium sulfate, sodium chloride and polyethylene glycol and spanned the pH range 4.6–8.5. Thus, proline is compatible with typical protein-crystallization formulations. The proline concentration needed for cryoprotection of these crystals is in the range 2.0–3.0 *M*. Complete data sets were collected from the proline-protected crystals. Proline performed as well as traditional cryoprotectants based on the diffraction resolution and data-quality statistics. The structures were refined to assess the binding of proline to these proteins. As observed with traditional cryoprotectants such as glycerol and ethylene glycol, the electron-density maps clearly showed the presence of proline molecules bound to the protein. In two cases, histidine acid phosphatase and 1-pyrroline-5-carboxylate dehydrogenase, proline binds in the active site. It is concluded that L-proline is an effective cryoprotectant for protein crystallography.

1. Introduction

X-ray diffraction data collection at cryogenic temperatures (~100 K) is nearly universal in macromolecular crystallography today. As water occupies a substantial fraction (~0.5) of the volume of macromolecular crystals, crystalline ice typically forms upon exposure of the untreated protein crystal to cryogenic temperatures. Crystalline ice can degrade diffraction quality, and the intense powder diffraction rings from microcrystalline ice compromise the adjacent protein reflections. This problem is typically prevented by adding a high concentration of a solute, known as the cryoprotectant, to the mother liquor or stabilizing solution (Hope, 2001). Commonly used cryoprotectants include glycerol, ethylene glycol, 2-methyl-2,4-pentanediol, low-molecular-weight polyethylene glycols (PEGs) and sucrose (Garman & Owen, 2007; Rodgers, 1997; Pflugrath, 2004). Lithium salts and sodium malonate can also be used as cryoprotectants in some cases (Rubinson *et al.*, 2000; Holyoak *et al.*, 2003). More recently,

Table 1
Proline-based cryobuffers.

	Lysozyme	XI-1	XI-2	FtHAP	Mm5CDH
Buffer	0.1 *M* Na acetate	0.1 *M* Tris–HCl	0.1 *M* Tris–HCl	0.1 *M* bis-Tris	0.1 *M* bis-Tris
pH	4.6	8.5	8.5	6.5	6.25
Precipitant	1.2 *M* NaCl	2.0 *M* $(NH_4)_2SO_4$	5% PEG 4000	2.0 *M* $(NH_4)_2SO_4$	25% PEG 3350
Proline (*M*)	2.8	2.0	3.0	2.0	2.4

the osmolytes trimethylamine *N*-oxide, sarcosine and betaine have been used successfully as cryoprotective agents for protein crystals (Mueller-Dieckmann *et al.*, 2011; Marshall *et al.*, 2012).

A motivation for the current study is nature's use of the amino acid L-proline as a cryoprotectant. Plants accumulate proline in response to environmental stresses, including freezing temperatures (Hare *et al.*, 1999; Yoshiba *et al.*, 1997; Szabados & Savouré, 2010). For example, early studies on coastal bermudagrass shoots showed that drought stress caused an increase of proline from less than 0.1 mg per gram of dry weight to over 15 mg per gram (Barnett & Naylor, 1966). Also, a 500-fold increase in free proline to levels as high as 60 m*M* has been observed in water-stressed tomato-plant cells (Handa *et al.*, 1983). Proline also protects yeast against freeze stress (Takagi, 2008; Morita *et al.*, 2002; Takagi *et al.*, 2000). Gene-knockout studies have shown that disruption of proline catabolism in yeast improves freeze tolerance and that the mutant yeast strains accumulate up to 9% of the cell's dry weight in proline (Takagi *et al.*, 2000). In addition, the freeze tolerance of certain fly larva is a consequence of elevated levels of proline (Koštál *et al.*, 2011, 2012). In some cold-acclimated larvae, for example, the proline concentration reaches 147 m*M* (Koštál *et al.*, 2011).

The role of proline in freeze tolerance *in vivo* has prompted the use of the amino acid in the cryopreservation of biological samples *in vitro*. For example, cultured cells of maize have been freeze-preserved in 10%(*w*/*v*) proline (Withers & King, 1979). Also, proline at 27 m*M* has been used for the preservation of ram sperm (Sánchez-Partida *et al.*, 1998). Additionally, low levels of proline [1%(*w*/*v*)] have been used in conjunction with other solutes in the cryopreservation of human stem cells (Freimark *et al.*, 2011). To our knowledge, proline has not been used as a cryoprotectant for protein crystals.

Here, we demonstrate the use of proline in the cryoprotection of crystals of hen egg-white lysozyme, xylose isomerase, histidine acid phosphatase and 1-pyrroline-5-carboxylate dehydrogenase. Proline was found to perform as well as traditional cryoprotectants in these cases.

2. Materials and methods

2.1. Loop diffraction tests

Loop diffraction tests were performed to determine the proline concentration range needed to prevent the formation of crystalline ice in the presence of the two common precipitants ammonium sulfate and PEG 3350. For these tests, stock solutions of 6.5 *M* proline, 4 *M* ammonium sulfate and 50%(*w*/*v*) PEG 3350 in water were prepared. We note that the pH of 6.5 *M* aqueous proline is 6.5. Several solutions containing various concentrations of proline and either ammonium sulfate or PEG 3350 were then made by mixing appropriate volumes of the stock solutions and water. Hampton Research 20 µm diameter nylon loops (0.5 mm loop size) were dipped into these solutions, flash-cooled in a cryogenic gaseous N_2 stream (Riguku X-stream 2000 set at 123 K) and exposed to X-rays from a Rigaku RUH3R rotating-anode source coupled to an R-AXIS IV^{++} detector. The cryostream was blocked with a thin plastic card while the loop was mounted on the goniometer and the card was quickly removed after the sample was in place. The loops were not blotted prior to transfer to the goniometer. The crystal-to-detector distance was 150 mm, which corresponds to 2.00 Å resolution at the detector edge. The exposure time was 1 min. Each solution was tested three times to ensure reproducibility.

2.2. Crystallization and cryoprotection

2.2.1. General cryoprotection procedure. The crystals were cryoprotected using the *in situ* serial transfer method described previously (Garman & Owen, 2007). In our implementation of this method, cryoprotection is initiated by adding 20–40 µl of a buffer containing a low concentration of the cryoprotectant to the sitting drop in which the crystal was grown (Cryschem plate). The solution bathing the crystal is then mixed by drawing 20 µl liquid into the pipette and expelling it back into the drop 3–5 times. Next, 20 µl buffer is removed, 20 µl fresh buffer is added and the solution is mixed. The cycle of removal, replacement and mixing is repeated until schlieren lines are no longer evident upon the addition of fresh buffer (typically 3–5 cycles). The entire procedure is repeated using a series of buffers with increasing amounts of the cryoprotectant until the final desired level of cryoprotectant is achieved. The time for cryoprotection was 5–10 min per crystal.

The cryoprotected crystals were picked up with Hampton Research 20 µm nylon loops and vitrified by plunging them into liquid nitrogen. The crystals were not blotted prior to plunging into liquid nitrogen, nor was the cold gas layer above the liquid-nitrogen surface removed (Warkentin *et al.*, 2006). The thickness of the cold gas layer was estimated to be 1–2 cm.

2.2.2. Lysozyme. Hen egg-white lysozyme (HEWL) was purchased from Sigma–Aldrich (catalogue No. L7651) and a stock solution of 12.5 mg ml^{-1} HEWL in 0.1 *M* sodium acetate buffer pH 4.6 was prepared. Tetragonal crystals were grown in 6 µl sitting drops (Cryschem plates) at room temperature using a reservoir solution consisting of 0.5–0.9 *M* NaCl, 0.1 *M* sodium acetate pH 4.6. The protein:reservoir ratio in the drop

was varied, with the largest crystals obtained at ratios of 4:2 and 3:3. HEWL crystals were cryoprotected in 2.8 *M* proline, 1.2 *M* NaCl, 0.1 *M* sodium acetate pH 4.6 (Table 1) *via* the *in situ* serial transfer method described above. The starting buffer was 0.5 *M* proline, 1.2 *M* NaCl, 0.1 *M* sodium acetate pH 4.6. The proline concentration in the buffer was increased stepwise to 1.0, 1.5, 2.0, 2.5 and finally 2.8 *M*.

As a control, HEWL crystals were also cryoprotected in ethylene glycol, a cryoprotectant that has previously been used with tetragonal HEWL crystals (Evans & Bricogne, 2002; Retailleau & Prangé, 2003). The starting buffer for *in situ* serial transfer cryoprotection was 10%(*v*/*v*) ethylene glycol, 0.9 *M* NaCl, 0.1 *M* sodium acetate pH 4.6. The ethylene glycol concentration was increased stepwise to 15, 20 and finally 22.5%.

2.2.3. Xylose isomerase. Xylose isomerase (XI) from *Streptomyces rubiginosus* was purchased from Hampton Research (catalogue No. HR7-102) as a crystalline suspension at 33 mg ml^{-1}. The protein was dialyzed into 10 m*M* HEPES, 1 m*M* $MgCl_2$ pH 7.0 and was concentrated to 25 mg ml^{-1} using a centrifugal device. Crystals were grown at room temperature in Cryschem sitting-drop plates using drops formed by mixing 1.5 µl each of the protein and reservoir solutions.

The *I*222 crystal form of XI was grown using a reservoir solution consisting of 1.0–2.2 *M* ammonium sulfate, 0.1 *M* Tris–HCl pH 7.0–8.5. The crystals were cryoprotected using the *in situ* stepwise approach described in §2.2.1. The starting buffer consisted of 1.0 *M* proline, 2.0 *M* ammonium sulfate, 0.1 *M* Tris–HCl pH 8.5. The proline concentration in the buffer was increased by 1.0 *M* in one step to achieve a final cryobuffer of 2.0 *M* proline, 2.0 *M* ammonium sulfate, 0.1 *M* Tris–HCl pH 8.5 (Table 1; XI-1).

For comparison purposes, XI crystals were also cryoprotected in glycerol. We note that glycerol has been used previously for *I*222 crystals of XI grown in ammonium sulfate (PDB entry 2glk). The starting buffer for *in situ* serial transfer cryoprotection was 5%(*v*/*v*) glycerol, 2.0 *M* ammonium sulfate, 0.2 *M* $MgCl_2$, 0.1 *M* Tris pH 8.0. The concentration of glycerol in the buffer was increased to 20% in steps of 5%.

The *I*222 crystal form of XI was also obtained using low ionic strength conditions consisting of 4–9%(*w*/*v*) PEG 4000, 0.2 *M* $MgCl_2$, 0.1 *M* Tris–HCl pH 7.0–8.5. The crystals were cryoprotected *in situ* by first replacing the mother liquor with 20 µl 1.0 *M* proline, 5%(*w*/*v*) PEG 4000, 0.2 *M* $MgCl_2$, 0.1 *M* Tris pH 8.5. The proline concentration was increased in 0.5 *M* steps to a final cryobuffer of 3.0 *M* proline, 5% PEG 4000, 0.2 *M* $MgCl_2$, 0.1 *M* Tris pH 8.5 (Table 1; XI-2). As a control experiment, this crystal form of XI was also cryoprotected in PEG 200. The starting buffer for cryoprotection was 5%(*v*/*v*) PEG 200, 5%(*w*/*v*) PEG 4000, 0.2 *M* $MgCl_2$, 0.1 *M* Tris pH 8.0. The PEG 200 concentration in the buffer was increased to 20% in steps of 5%.

2.2.4. Histidine acid phosphatase. The H17N/D261A double mutant of the histidine acid phosphatase from *Francisella tularensis* (FtHAP) was expressed using auto-induction (Studier, 2005) and was purified and crystallized as described previously (Felts *et al.*, 2006; Singh *et al.*, 2009).

Table 2
Data-collection and refinement statistics for HEWL.

Values in parentheses are for the outer resolution shell.

Cryoprotectant	2.8 *M* proline	22.5% ethylene glycol
Space group	$P4_32_12$	$P4_32_12$
Unit-cell parameters (Å)	$a = b = 78.0$, $c = 37.7$	$a = b = 78.9$, $c = 36.9$
Wavelength (Å)	1.54	1.54
Resolution (Å)	19.50–1.50 (1.58–1.50)	19.50–1.50 (1.58–1.50)
No. of observations	205088	228617
Unique reflections	19076	19082
$R_{merge}(I)$	0.028 (0.241)	0.028 (0.148)
$R_{meas}(I)$	0.029 (0.257)	0.029 (0.157)
$R_{p.i.m.}(I)$	0.008 (0.085)	0.008 (0.051)
Mean $I/\sigma(I)$	46.1 (7.6)	58.6 (12.9)
Completeness (%)	99.6 (97.6)	99.9 (99.5)
Multiplicity	10.8 (8.2)	12.0 (8.8)
Mosaicity (°)	0.21	0.13
No. of protein atoms	976	
No. of water molecules	99	
No. of proline molecules	1	
R_{cryst}	0.185	
R_{free}†	0.216	
R.m.s. deviations‡		
Bond lengths (Å)	0.005	
Bond angles (°)	1.012	
Ramachandran plot§, residues in		
Favored regions	126	
Allowed regions	1	
Outliers	0	
Average *B* factor (Å^2)		
Protein	16	
Water	25	
Proline	22	
PDB code	4e3u	

† 5% test set. ‡ Compared with the parameters of Engh & Huber (1991). § The Ramachandran plot was generated with *RAMPAGE* (Lovell *et al.*, 2003).

Crystals were grown in sitting drops using a reservoir solution consisting of 1.7–2.2 *M* ammonium sulfate, 0.1 *M* bis-Tris pH 5.5–6.5. The drop size was 2 µl and equal volumes of the protein and reservoir solutions were mixed. The space group of the crystals was $P4_1$, with unit-cell parameters $a = b = 62.0$, $c = 210.4$ Å. The starting buffer for *in situ* cryoprotection was 1.0 *M* proline, 2.0 *M* ammonium sulfate, 0.1 *M* bis-Tris pH 6.5. The proline concentration was increased in 0.5 *M* steps to a final cryobuffer of 2.0 *M* proline, 2.0 *M* ammonium sulfate, 0.1 *M* bis-Tris pH 6.5 (Table 1).

For comparison purposes, FtHAP crystals were also cryoprotected in glycerol as described previously (Singh *et al.*, 2009). The starting buffer for cryoprotection was 5%(*v*/*v*) glycerol, 2.0 *M* ammonium sulfate, 0.1 *M* bis-Tris pH 6.25. The glycerol concentration was increased using *in situ* serial transfer to 10, 15 and finally 20%.

2.2.5. 1-Pyrroline-5-carboxylate dehydrogenase. 1-Pyrroline-5-carboxylate dehydrogenase from *Mus musculus* (MmP5CDH) was expressed, purified and crystallized as recently described (Srivastava *et al.*, 2012). MmP5CDH was crystallized using a reservoir consisting of 15–25% PEG 3350, 0.1 *M* bis-Tris pH 5.5–6.5. The space group of the crystals was $P2_12_12_1$, with unit-cell parameters $a = 84.9$, $b = 94.0$, $c = 132.4$ Å. The reservoir solution served as the initial buffer for *in situ* stepwise cryoprotection. Cryoprotection was achieved in a

Table 3
Data-collection and refinement statistics for XI.

Values in parentheses are for the outer resolution shell.

	XI-1-pro	XI-1-gol	XI-2-pro	XI-2-peg
Cryoprotectant	2.0 *M* proline	20% glycerol	3.0 *M* proline	20% PEG 200
Space group	*I*222	*I*222	*I*222	*I*222
Unit-cell parameters (Å)	a = 92.5, b = 98.0, c = 102.4	a = 92.5, b = 98.2, c = 101.8	a = 92.8, b = 98.1, c = 102.7	a = 93.0, b = 97.8, c = 102.9
Wavelength (Å)	1.54	1.54	1.54	1.54
Resolution (Å)	19.5–1.50 (1.58–1.50)	19.5–1.50 (1.58–1.50)	19.7–1.50 (1.58–1.50)	19.7–1.50 (1.58–1.50)
No. of observations	470488	490567	463654	487593
Unique reflections	72416	72675	73511	73858
$R_{\rm merge}(I)$	0.037 (0.183)	0.071 (0.552)	0.037 (0.174)	0.046 (0.160)
$R_{\rm meas}(I)$	0.040 (0.203)	0.077 (0.608)	0.040 (0.194)	0.500 (0.178)
$R_{\rm p.i.m.}(I)$	0.015 (0.085)	0.029 (0.249)	0.016 (0.082)	0.019 (0.076)
Mean $I/\sigma(I)$	30.1 (8.5)	20.6 (3.1)	31.3 (8.7)	27.5 (9.2)
Completeness (%)	97.8 (89.5)	98.5 (93.1)	98.8 (92.2)	99.0 (94.2)
Multiplicity	6.5 (5.2)	6.8 (5.4)	6.3 (4.9)	6.6 (4.8)
Mosaicity (°)	0.19	0.25	0.13	0.12
No. of protein atoms	3052		3086	
No. of water molecules	324		292	
No. of proline molecules	1		0	
$R_{\rm cryst}$	0.164		0.172	
$R_{\rm free}$†	0.179		0.187	
R.m.s. deviations‡				
Bond lengths (Å)	0.006		0.006	
Bond angles (°)	1.107		1.066	
Ramachandran plot§, residues in				
Favored regions	372		373	
Allowed regions	10		12	
Outliers	1		1	
Average B factor (Å^2)				
Protein	11		10	
Water	21		17	
Proline	20		—	
PDB code	4e3v			

† 5% test set. ‡ Compared with the parameters of Engh & Huber (1991). § The Ramachandran plot was generated with *RAMPAGE* (Lovell *et al.*, 2003).

single step with a final buffer of 2.4 *M* proline, 25% PEG 3350, 0.1 *M* bis-Tris pH 6.25 (Table 1).

2.3. Data collection and refinement

X-ray diffraction data were collected from the HEWL and XI crystals using a rotating-anode X-ray source and an R-AXIS IV^{++} detector. For each data set, the crystal-to-detector distance was 85 mm, the exposure time was 2 min per frame and the oscillation width was 0.5°. The resolution of the inscribed circle of the detector at 85 mm is 1.52 Å.

Data from FtHAP crystals were collected on beamline 4.2.2 of the Advanced Light Source using a NOIR-1 detector. Each data set consisted of 546 images with a crystal-to-detector distance of 160 mm, a detector offset of 8°, an oscillation width of 0.33° and an exposure time of 2 s per frame. The resolution limits at the top and bottom edges of the detector were 1.72 and 3.21 Å, respectively, while the resolution at the side of the detector was 2.25 Å.

Data from an MmP5CDH crystal were collected on beamline 24-ID-E of the Advanced Photon Source using an ADSC Q315 detector. The data set was collected using a continuous vector scan and consisted of 120 images obtained using a crystal-to-detector distance of 125 mm, an oscillation width of 1.0° and an exposure time of 1 s per frame at 100% transmittance. The resolution of the inscribed circle of the detector was 1.10 Å.

All data sets were integrated with *XDS* (Kabsch, 2010) and scaled with *SCALA* (Evans, 2006) *via* the *CCP*4*i* interface (Potterton *et al.*, 2003). Data-collection statistics are listed in Tables 2, 3, 4 and 5. The mosaicity values in Tables 2–5 are from the CORRECT step of *XDS*.

The data sets were used in structure refinement in order to identify proline molecules bound to the protein. Refinement was performed with *PHENIX* (Adams *et al.*, 2010) starting from coordinates derived from the following structures: HEWL, PDB entry 2lyz (Diamond, 1974); XI, PDB entry 1xif (Carrell *et al.*, 1994); FtHAP, PDB entry 3it2 (Singh *et al.*, 2009); MmP5CDH, PDB entry 3v9j (Srivastava *et al.*, 2012). In each case solvent molecules were removed prior to refinement. The refinement protocol consisted of rigid-body refinement followed by simulated annealing. The *B*-factor model consisted of an isotropic *B* factor for each non-H atom plus one TLS group per protein chain for HEWL, XI and FtHAP. Anisotropic *B* factors were used for the refinement of MmP5CDH. After the first round of refinement, *Coot* (Emsley & Cowtan, 2004) was used to adjust the protein model and to add water molecules. The model was then input to *PHENIX* for a second round of refinement. The resulting electron-density maps were inspected, proline molecules were added

Table 4
Data-collection and refinement statistics for FtHAP.

Values in parentheses are for the outer resolution shell.

Cryoprotectant	2.0 *M* proline	20% glycerol
Space group	$P4_1$	$P4_1$
Unit-cell parameters (Å)	$a = b = 62.0$, $c = 210.4$	$a = b = 62.0$, $c = 211.0$
Wavelength (Å)	1.00	1.00
Resolution (Å)	48.6–1.75 (1.84–1.75)	46.5–1.75 (1.84–1.75)
No. of observations	341312	308938
Unique reflections	78960	76942
$R_{\rm merge}(I)$	0.032 (0.130)	0.065 (0.153)
$R_{\rm meas}(I)$	0.036 (0.160)	0.072 (0.199)
$R_{\rm p.i.m.}(I)$	0.015 (0.092)	0.030 (0.126)
Mean $I/\sigma(I)$	25.8 (5.7)	13.1 (3.1)
Completeness (%)	99.1 (95.3)	96.6 (81.1)
Multiplicity	4.3 (2.8)	4.0 (1.9)
Mosaicity (°)	0.18	0.24
No. of protein atoms	5035	
No. of water molecules	365	
No. of proline molecules	2	
$R_{\rm cryst}$	0.182	
$R_{\rm free}$†	0.203	
R.m.s. deviations‡		
Bond lengths (Å)	0.006	
Bond angles (°)	1.007	
Ramachandran plot§, residues in		
Favored regions	648	
Allowed regions	6	
Outliers	0	
Average *B* factor (Å^2)		
Protein	19	
Water	23	
Proline	24	
PDB code	4e3w	

† 5% test set. ‡ Compared with the parameters of Engh & Huber (1991). § The Ramachandran plot was generated with *RAMPAGE* (Lovell *et al.*, 2003).

Table 5
Data-collection and refinement statistics for MmP5CDH.

Values in parentheses are for the outer resolution shell.

Cryoprotectant	2.4 *M* proline
Space group	$P2_12_12_1$
Unit-cell parameters (Å)	$a = 85.0$, $b = 93.9$, $c = 132.4$
Wavelength (Å)	0.979
Resolution (Å)	45.6–1.24 (1.31–1.24)
No. of observations	1144056
Unique reflections	279378
$R_{\rm merge}(I)$	0.051 (0.550)
$R_{\rm meas}(I)$	0.058 (0.644)
$R_{\rm p.i.m.}(I)$	0.027 (0.326)
Mean $I/\sigma(I)$	15.0 (2.3)
Completeness (%)	94.1 (87.3)
Multiplicity	4.1 (3.3)
Mosaicity (°)	0.17
No. of protein atoms	8304
No. of water molecules	882
No. of proline molecules	7
$R_{\rm cryst}$	0.155
$R_{\rm free}$†	0.180
R.m.s. deviations‡	
Bond lengths (Å)	0.005
Bond angles (°)	1.078
Ramachandran plot§, residues in	
Favored regions	1066
Allowed regions	19
Outliers	0
Average *B* factor (Å^2)	
Protein	12
Water	22
Proline	18
PDB code	4e3x

† 5% test set. ‡ Compared with the parameters of Engh & Huber (1991). § The Ramachandran plot was generated with *RAMPAGE* (Lovell *et al.*, 2003).

and *PHENIX* refinement was performed. This procedure was repeated as necessary. Refinement statistics are listed in Tables 2–5. Coordinates and structure factors for structures containing ordered proline molecules have been deposited in the PDB under the accession codes listed in Tables 2–5.

3. Results

3.1. Loop diffraction tests

Loop diffraction tests were performed to determine the proline concentration range needed for cryoprotection. A solution of 4 *M* proline prevents crystalline ice rings; lower proline levels afford cryoprotection when other solutes are present. In particular, Fig. 1 shows diffraction images from loops containing 1.0–3.0 *M* proline together with one of two common precipitants: ammonium sulfate (Fig. 1*a*) or PEG 3350 (Fig. 1*b*).

The data for mixtures of proline and ammonium sulfate suggest that the sum of the two solute concentrations should be at least 4 *M* to prevent crystalline ice formation (Fig. 1*a*). For example, a combination of 2.0 *M* ammonium sulfate and 2.0 *M* proline prevents crystalline ice formation. The diffraction pattern from a solution of 1.0 *M* ammonium sulfate and 3.0 *M* proline is also free of crystalline ice rings, but rings are evident when the proline concentration is lowered to 2.5 *M*. Likewise, a solution of 1.5 *M* ammonium sulfate and 2.5 *M* proline is cryoprotective, but a combination of 1.5 *M* ammonium sulfate and 2.0 *M* proline does not prevent crystalline ice formation.

Solutions containing proline and PEG 3350 were also tested (Fig. 1*b*). Crystalline ice formation is suppressed by 15%(*w*/*v*) PEG 3350 and 2.5 *M* proline. If the PEG concentration is increased to 20% the proline concentration may be decreased to 2.0 *M*. Increasing the PEG concentration further to 25% allows the proline concentration to be lowered to 1.5 *M*. Thus, a rule of thumb is that 0.5 *M* proline is roughly equivalent to 5% PEG 3350 in terms of cryoprotective capacity.

3.2. Diffraction data

HEWL is a standard test case for protein-crystallography methods development; therefore, we tested proline cryoprotection of HEWL crystals. A diffraction data set was collected from a HEWL crystal that had been cryoprotected in 2.8 *M* proline. To facilitate the assessment of proline as a cryoprotectant, a comparison data set was collected from another crystal that had been cryoprotected in 22.5% ethylene glycol. Both crystals diffracted to beyond 1.5 Å resolution using a rotating-anode source and the data sets were truncated at 1.5 Å resolution owing to the limitation of the minimum detector distance on our system (Table 2). The mosaicity of the proline-soaked crystal was about 50% higher than that

of the ethylene glycol-soaked crystal. Otherwise, the two data sets were comparable in terms of global indicators of quality such as $R_{\rm merge}$, $R_{\rm meas}$, $R_{\rm p.i.m.}$ and $\langle I/\sigma(I)\rangle$. It is difficult to know whether such small differences in data-quality statistics are a consequence of the cryoprotectant or simply reflect crystal-to-crystal variation. Nevertheless, these data certainly show that proline does not substantially degrade the diffraction characteristics of HEWL crystals, which suggests that proline is a potentially promising cryoprotectant. Thus, proline passes the lysozyme test.

XI is another test case that is routinely used for methods development. The *I*222 form of XI was grown under two different conditions corresponding to high (XI-1) and low (XI-2) ionic strength. XI-1 crystals were cryoprotected in 2.0 *M* proline and a data set was collected using a rotating-anode system (Table 3; XI-1-pro). A comparison data set was collected from an XI-1 crystal that had been cryoprotected in 20% glycerol (Table 3; XI-1-gol). Similarly, data sets from XI-2 crystals cryoprotected in proline (Table 3; XI-2-pro) and PEG 200 (Table 3; XI-2-peg) were also obtained. All four crystals diffracted to beyond 1.50 Å resolution. The mosaicities of the XI-1 crystals are about 0.2°, whereas those of the XI-2 crystals are 0.1°. The data-quality statistics are very similar for the XI-1-pro, XI-2-pro and XI-2-peg data sets. Interestingly, those for the XI-1-gol data set are noticeably worse. In particular, the *R* factors of this data set are about two times higher than those of the other three data sets. Likewise, the $\langle I/\sigma(I)\rangle$ for XI-1-gol is substantially lower (Table 3). These differences are most evident in the high-resolution bin. As with the HEWL data, it is difficult to know whether these differences reflect crystal variation or the cryoprotectant. However, the data appear to suggest that proline performs as well as PEG 200 for XI-2 crystals and possibly better than glycerol for XI-1 crystals.

In addition to the two above-mentioned test cases, we investigated two other proteins available in our laboratory: FtHAP and MmP5CDH. FtHAP was crystallized at high ionic strength with ammonium sulfate, whereas MmP5CDH crystals grew at lower ionic strength with PEG 3350 as the precipitant. Thus, these two cases represent quite different regions of crystallization space and provide an opportunity to assess the generality of proline as a cryoprotectant.

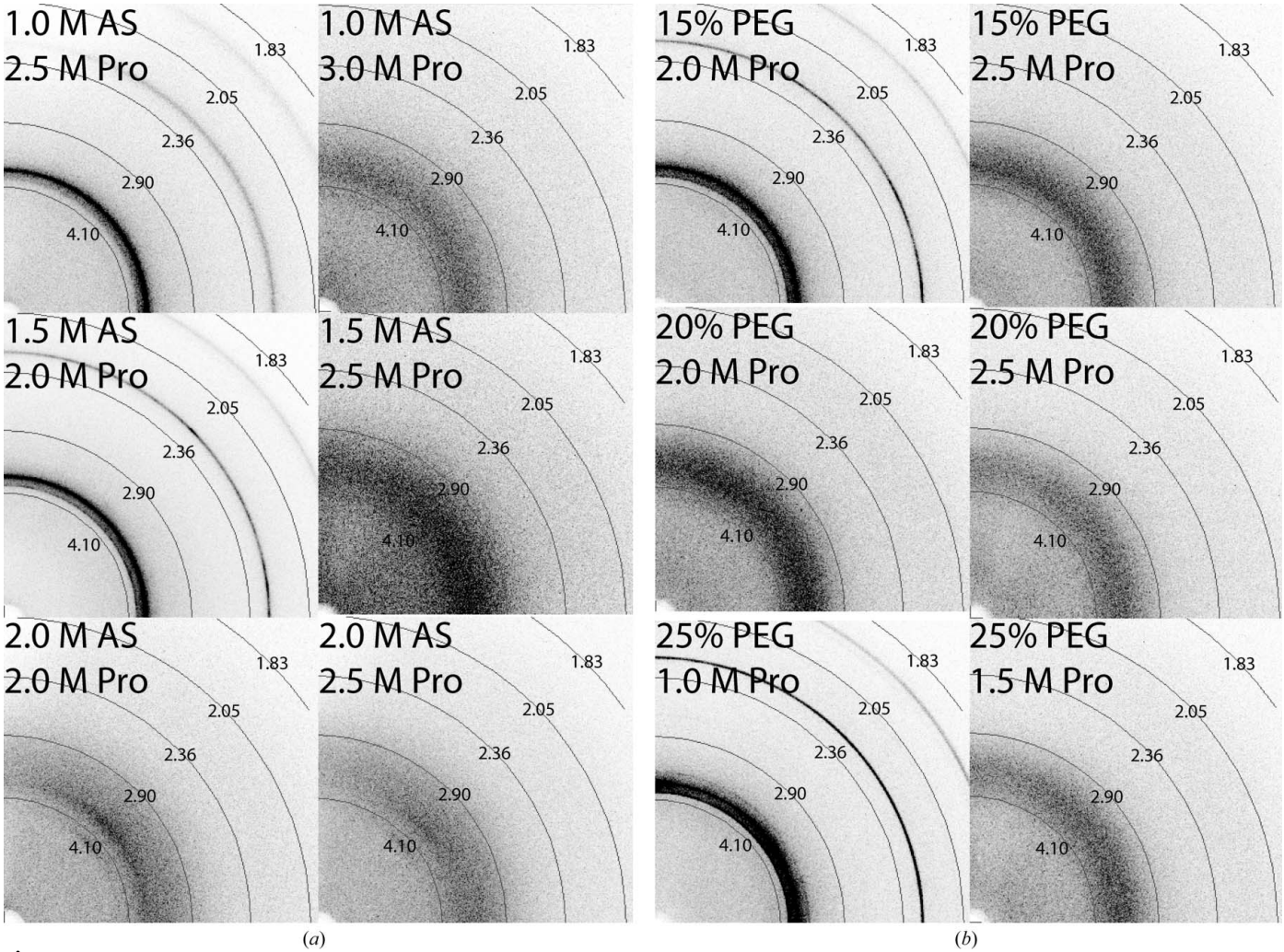

Figure 1
X-ray diffraction images from loops containing proline (Pro) and either (*a*) ammonium sulfate (AS) or (*b*) PEG 3350 (PEG). The crystal-to-detector distance is 150 mm for all images. Resolution arcs are indicated in Å.

Data from a proline-soaked FtHAP crystal were collected on Advanced Light Source beamline 4.2.2 (Table 4). Another data set using identical data-collection parameters was collected from a crystal that was cryoprotected in glycerol (Table 4). Both data sets were processed to 1.75 Å resolution. Although it is difficult to account for the effects of crystal-to-crystal variation, the data seem to suggest that proline is superior to glycerol for cryoprotecting FtHAP crystals. For example, the mosaicity of the proline-soaked crystal (0.18°) is slightly lower than that of the glycerol-soaked crystal (0.24°). Furthermore, the *R* factors for the proline data set are about half those for the glycerol data set. Also, the $\langle I/\sigma(I)\rangle$ of the proline data is about twice that of the glycerol data. These results suggest that proline is a good cryoprotectant for FtHAP crystals.

Finally, a 1.24 Å resolution data set was collected on Advanced Photon Source beamline 24-ID-E from a crystal of MmP5CDH that was cryoprotected in 2.4 *M* proline (Table 5). For reference, we have recently reported structures of MmP5CDH complexed with sulfate ion, the product glutamate and the cofactor NAD^+ which were determined from crystals that were cryoprotected in 25% glycerol (Srivastava *et al.*, 2012). The high-resolution limits of those structures ranged from 1.30 Å for the sulfate complex to 1.50 Å for the glutamate and NAD^+ complexes. The mosaicity of the proline-soaked crystal is 0.17°, whereas the mosaicities of the glycerol-soaked crystals were 0.12–0.15°. Thus, soaking with proline did not degrade the resolution or substantially increase the mosaicity of MmP5CDH crystals.

3.3. Ordered proline molecules

Electron-density maps were inspected to identify ordered proline molecules bound to the protein and this analysis clearly indicated that proline molecules were bound to all four enzymes (Tables 2–5). One proline molecule binds to HEWL in a crystal contact region formed by residues 19, 22 and 24 of one protein and Arg114 of a symmetry-related protein (Supplementary Fig. S1[1]). One proline site was also identified for XI. Electron density for proline was observed at this location in both crystal forms, but the density was much stronger in the ammonium sulfate form (XI-1-pro). Proline binds in a water-filled trough on the surface of XI and interacts with Ser281 (Supplementary Fig. S2[1]).

The active site of FtHAP contains one proline molecule, which is wedged between Phe23 and Tyr135 and forms no direct hydrogen bonds to the enzyme (Fig. 2). Interestingly, Phe23 and Tyr135 form an aromatic clamp that binds the adenine base of the substrate 3′-AMP (Singh *et al.*, 2009). As shown in Fig. 2(*b*), the proline molecule occupies the substrate adenine site. A sulfate ion is also bound in the active site and occupies the substrate phosphoryl binding pocket. Thus, proline and sulfate together appear to mimic the substrate 3′-AMP.

Seven proline molecules are bound to MmP5CDH (Fig. 3). Three prolines are bound to each of the two proteins in the asymmetric unit (labeled 1, 2 and 3 in Fig. 3) and an additional proline binds in a crystal contact (labeled 4 in Fig. 3). Proline 1 binds in the active site and forms hydrogen bonds to Gly512 and Ser513 (Fig. 3, inset 1). The electron density suggests that the bound proline possibly exhibits conformational disorder or has less than full occupancy. Interestingly, this location corresponds to the binding site for the aldehyde substrate (and the glutamate product; Srivastava *et al.*, 2012). In fact, the backbone of the bound proline superimposes almost perfectly with that of the product glutamate (Fig. 3, inset 1). That proline binds in this site is consistent with the fact that proline is a competitive inhibitor of P5CDH (Forte-McRobbie & Pietruszko, 1989). Proline 2 binds in the crevice between the NAD^+-binding and catalytic lobes and forms electrostatic

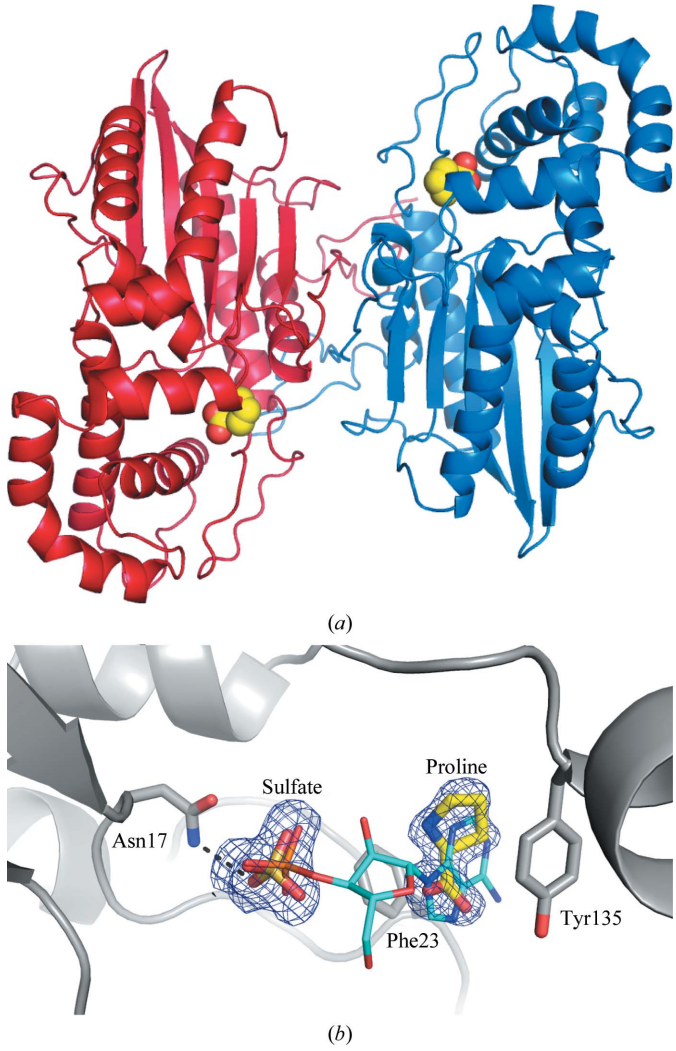

Figure 2
Proline bound to the active site of FtHAP. (*a*) Ribbon drawing of the dimer with the bound proline molecules drawn as spheres. (*b*) Electron density for proline bound to the active site of FtHAP. The cage represents a simulated-annealing σ_A-weighted $F_o - F_c$ OMIT map contoured at 3.0σ. The substrate 3′-AMP bound to FtHAP mutant D261A (PDB entry 3it3) is shown as thin cyan sticks. This figure and others were created with *PyMOL* (DeLano, 2002).

[1] Supplementary material has been deposited in the IUCr electronic archive (Reference: DW5018). Services for accessing this material are described at the back of the journal.

interactions with Arg399 and Asp393 (Fig. 3, inset 2). Also, the nonpolar part of the pyrrolidine ring of proline 2 contacts Phe210. Proline 3 contacts both protomers of the dimer (Fig. 3). Proline 3 forms electrostatic interactions with Lys292 of one chain and the 303–308 loop of the other chain (Fig. 3, inset 3). Also, the pyrrolidine ring of proline 3 makes nonpolar contacts with Leu302 and Phe308 of one chain of the dimer and Ala525 of the other chain. Finally, proline 4 binds in a crystal contact region. This proline interacts with the backbone of Gln184 of the protein in the asymmetric unit and is linked *via* two water molecules to Glu46 of a symmetry-related molecule (Fig. 3, inset 4).

4. Discussion

The results reported here suggest that proline is a suitable cryoprotectant for protein crystals. Our test cases included two 'model' proteins, HEWL and XI, as well as a phosphatase and an aldehyde dehydrogenase. None of these crystals exhibited any signs of deterioration, such as cracking or melting, while soaking with proline. Furthermore, the diffraction images obtained from these crystals were free of crystalline ice rings.

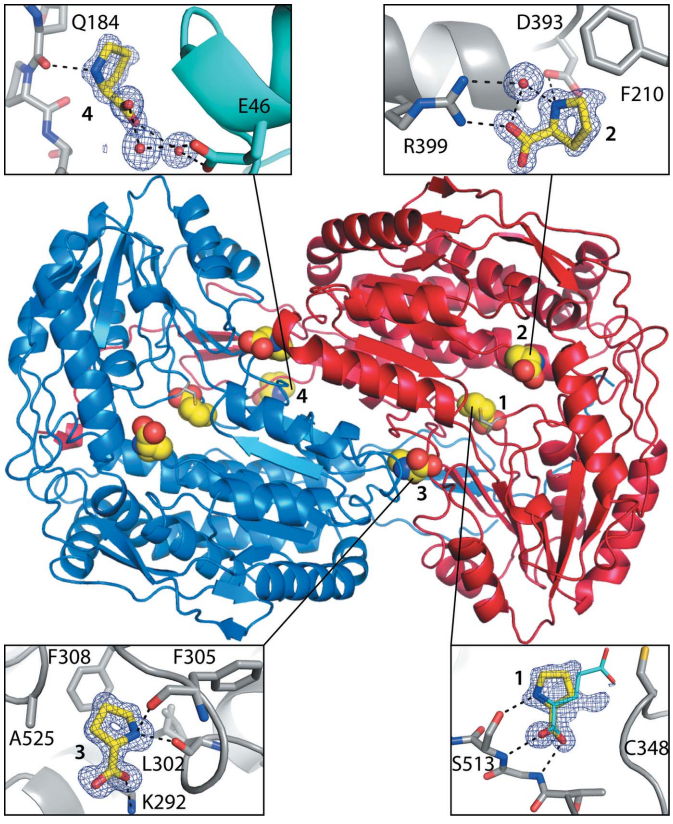

Figure 3
Proline molecules bound to Mm5CDH. The two protomers of the dimer are colored red and blue. Bound proline molecules are shown as yellow spheres. The insets show close-up views of the four proline-binding sites. The cage represents a simulated-annealing σ_A-weighted $F_o - F_c$ OMIT map contoured at 3.0σ. In inset 1, the product glutamate from the structure of MmP5CDH-Glu (PDB entry 3v9k) is shown as thin cyan sticks. In inset 4, the protein in the asymmetric unit is colored gray and the protein related by $(x - 1/2, -y + 1/2, -z)$ is colored cyan.

Moreover, the diffraction quality is similar to that obtained from crystals of these enzymes cryoprotected with conventional reagents such as ethylene glycol, glycerol and PEG 200.

The crystallization recipes of our test cases are representative of those used in protein crystallography. The precipitants include ammonium sulfate, NaCl and PEG 3350, which are commonly used in protein crystallization. The pH values of the crystallization solutions span a wide range: 4.6–8.5. Thus, proline is compatible with the kinds of solutions that are typically used in protein crystallization, suggesting that proline is widely applicable as a cryoprotectant for protein crystals.

Electron-density maps clearly indicated ordered proline molecules bound to the protein in four of the five crystal structures. This result is expected because penetrating cryoprotectants frequently bind to proteins. In fact, as of 29 April 2012 the PDB contained 6620 entries with glycerol as a ligand, 2720 entries with ethylene glycol as a ligand and 702 entries with 2-methyl-2,4-pentanediol as a ligand. Typically, these compounds are present at 10–30%(*v*/*v*) in the cryobuffer, which corresponds to 1–5 *M*. This concentration range is similar to that of proline used here (2.0–3.0 *M*). Furthermore, like glycerol, ethylene glycol and 2-methyl-2,4-pentanediol, proline has both hydrogen-bond donors and acceptors. The similarities of proline to traditional cryoprotection agents suggest that one should expect to find proline bound to the protein.

Finally, we note that we have not attempted to perform a systematic head-to-head comparison between proline and other cryoprotectants. Such a study is challenging because it is difficult to account for crystal-to-crystal variation of the diffraction quality. Rather, our goal was to demonstrate that proline is an effective and generally applicable cryoprotectant for protein crystals. Our data support this assertion.

This research was supported by NIH grant GM065546. We thank Dr Jay Nix and Dr Jonathan Schuermann for help with data collection and processing. Part of this research was performed at the Advanced Light Source. The Advanced Light Source is supported by the Director, Office of Science, Office of Basic Energy Sciences of the US Department of Energy under Contract No. DE-AC02-05CH11231. This work is based upon research conducted at the Advanced Photon Source on the Northeastern Collaborative Access Team beamlines, which are supported by award RR-15301 from the National Center for Research Resources at the National Institutes of Health. Use of the Advanced Photon Source, an Office of Science User Facility operated for the US Department of Energy (DOE) Office of Science by Argonne National Laboratory, was supported by the US DOE under Contract No. DE-AC02-06CH11357.

References

Adams, P. D. *et al.* (2010). *Acta Cryst.* D**66**, 213–221.
Barnett, N. M. & Naylor, A. W. (1966). *Plant Physiol.* **41**, 1222–1230.
Carrell, H. L., Hoier, H. & Glusker, J. P. (1994). *Acta Cryst.* D**50**, 113–123.
DeLano, W. L. (2002). *PyMOL*. http://www.pymol.org.

Diamond, R. (1974). *J. Mol. Biol.* **82**, 371–391.
Emsley, P. & Cowtan, K. (2004). *Acta Cryst.* D**60**, 2126–2132.
Engh, R. A. & Huber, R. (1991). *Acta Cryst.* A**47**, 392–400.
Evans, P. (2006). *Acta Cryst.* D**62**, 72–82.
Evans, G. & Bricogne, G. (2002). *Acta Cryst.* D**58**, 976–991.
Felts, R. L., Reilly, T. J., Calcutt, M. J. & Tanner, J. J. (2006). *Acta Cryst.* F**62**, 32–35.
Forte-McRobbie, C. & Pietruszko, R. (1989). *Biochem. J.* **261**, 935–943.
Freimark, D., Sehl, C., Weber, C., Hudel, K., Czermak, P., Hofmann, N., Spindler, R. & Glasmacher, B. (2011). *Cryobiology*, **63**, 67–75.
Garman, E. & Owen, R. L. (2007). *Methods Mol. Biol.* **364**, 1–18.
Handa, S., Bressan, R. A., Handa, A. K., Carpita, N. C. & Hasegawa, P. M. (1983). *Plant Physiol.* **73**, 834–843.
Hare, P. D., Cress, W. A. & van Staden, J. (1999). *J. Exp. Bot.* **50**, 413–434.
Holyoak, T., Fenn, T. D., Wilson, M. A., Moulin, A. G., Ringe, D. & Petsko, G. A. (2003). *Acta Cryst.* D**59**, 2356–2358.
Hope, H. (2001). *International Tables for Crystallography*, Vol. *F*, edited by M. G. Rossmann & E. Arnold, pp. 197–201. Dordrecht: Kluwer Academic Publishers.
Kabsch, W. (2010). *Acta Cryst.* D**66**, 125–132.
Koštál, V., Šimek, P., Zahradníčková, H., Cimlová, J. & Štětina, T. (2012). *Proc. Natl. Acad. Sci. USA*, **109**, 3270–3274.
Koštál, V., Zahradníčková, H. & Šimek, P. (2011). *Proc. Natl Acad. Sci. USA*, **108**, 13041–13046.
Lovell, S. C., Davis, I. W., Arendall, W. B. III, de Bakker, P. I., Word, J. M., Prisant, M. G., Richardson, J. S. & Richardson, D. C. (2003). *Proteins*, **50**, 437–450.
Marshall, H., Venkat, M., Hti Lar Seng, N. S., Cahn, J. & Juers, D. H. (2012). *Acta Cryst.* D**68**, 69–81.
Morita, Y., Nakamori, S. & Takagi, H. (2002). *J. Biosci. Bioeng.* **94**, 390–394.
Mueller-Dieckmann, C., Kauffmann, B. & Weiss, M. S. (2011). *J. Appl. Cryst.* **44**, 433–436.
Pflugrath, J. W. (2004). *Methods*, **34**, 415–423.
Potterton, E., Briggs, P., Turkenburg, M. & Dodson, E. (2003). *Acta Cryst.* D**59**, 1131–1137.
Retailleau, P. & Prangé, T. (2003). *Acta Cryst.* D**59**, 887–896.
Rodgers, D. W. (1997). *Methods Enzymol.* **276**, 183–203.
Rubinson, K. A., Ladner, J. E., Tordova, M. & Gilliland, G. L. (2000). *Acta Cryst.* D**56**, 996–1001.
Sánchez-Partida, L. G., Setchell, B. P. & Maxwell, W. M. (1998). *Reprod. Fertil. Dev*. **10**, 347–357.
Singh, H., Felts, R. L., Schuermann, J. P., Reilly, T. J. & Tanner, J. J. (2009). *J. Mol. Biol.* **394**, 893–904.
Srivastava, D., Singh, R. K., Moxley, M. A., Henzl, M. T., Becker, D. F. & Tanner, J. J. (2012). *J. Mol. Biol.* **420**, 176–189.
Studier, F. W. (2005). *Protein Expr. Purif.* **41**, 207–234.
Szabados, L. & Savouré, A. (2010). *Trends Plant Sci.* **15**, 89–97.
Takagi, H. (2008). *Appl. Microbiol. Biotechnol.* **81**, 211–223.
Takagi, H., Sakai, K., Morida, K. & Nakamori, S. (2000). *FEMS Microbiol. Lett.* **184**, 103–108.
Warkentin, M., Berejnov, V., Husseini, N. S. & Thorne, R. E. (2006). *J. Appl. Cryst.* **39**, 805–811.
Withers, L. A. & King, P. J. (1979). *Plant Physiol.* **64**, 675–678.
Yoshiba, Y., Kiyosue, T., Nakashima, K., Yamaguchi-Shinozaki, K. & Shinozaki, K. (1997). *Plant Cell Physiol.* **38**, 1095–1102.